Geometric Synthesis of Planar 3-*RPR* Parallel Mechanisms for Singularity-Free Workspace

Qimi Jiang[1], Clément M. Gosselin[2]

[1] *Département de Génie Mécanique, Université Laval, qimi.jiang.1@ulaval.ca*

[2] *Département de Génie Mécanique, Université Laval, gosselin@gmc.ulaval.ca*

Abstract This work focuses on the geometric synthesis of planar 3-*RPR* parallel mechanisms in order to guarantee a singularity-free workspace for a desired orientation range. The effects of the orientation angle, the minimal leg length as well as the base shape on the singularity-free workspace are analyzed using the Gauss divergence theorem. The results show that for every orientation angle, there exists an optimal minimal leg length which leads to the maximal singularity-free workspace. If the optimal minimal leg lengths are used, the equilateral triangle base yields the maximal singularity-free workspace for any orientation angle. However, for a prescribed working range of the orientation angle, the optimal minimal leg length may be different from the individual optimal minimal leg lengths. Based on the optimal minimal leg length determined for a prescribed working range of the orientation angle, a geometric synthesis procedure is proposed in order to guarantee a singularity-free workspace.

Keywords: Planar 3-*RPR* parallel mechanisms, Singularity-free workspace, Optimal minimal leg length, Geometric synthesis

Synthèse géométrique des mécanismes parallèles plans de type 3-*RPR* pour l'espace de travail libre de singularité

Résumé Ce travail se concentre sur la synthèse géométrique des mécanismes parallèles plans de type 3-*RPR* afin de garantir un espace de travail libre de singularité pour un débattement angulaire désiré. Les effets de l'orientation, de la longueur minimale des pattes ainsi que de la forme de la base sur la zone de travail libre de singularité sont analysés en utilisant le théorème de la divergence de Gauss. Les résultats prouvent que pour chaque angle d'orientation, il existe une longueur minimale optimale des pattes qui mène à la zone de travail libre de singularité maximale. Si les longueurs minimales optimales des pattes sont considérées, la base triangulaire équilaterale correspond à la zone de travail libre de singularité maximale pour n'importe quel angle d'orientation. Cependant, pour une plage d'orientation prescrite, la longueur minimale optimale des pattes peut être différente des longueurs minimales optimales individuelles des pattes. Basé sur la longueur minimale optimale des pattes déterminée pour un débattement angulaire prescrit, on propose une procédure de synthèse géométrique afin de garantir une zone de travail libre de singularité.

Mots clés: Mécanismes parallèles plans 3-*RPR*, Espace de travail libre de singularité, Longueur minimale optimale des pattes, Synthèse géométrique

1 INTRODUCTION

Parallel mechanisms possess remarkable advantages over serial mechanisms in terms of dynamic properties, load-carrying capacity, high accuracy as well as stiffness or stability. However, the closed-loop nature of their architecture limits the motion of the platform and creates complex kinematic singularities inside the workspace. Hence, avoiding singularities inside the workspace becomes a very important issue.

Basically, there are three types of singularities [1]. Among these three types, the second type of singularities — direct kinematic singularity — may occur inside the workspace and is thus a serious concern for robot designers. In order to avoid this type of singularities, deriving the singularity equations is the first and key step ([1]–[5]).

Planar 3-*R*P*R* parallel mechanisms were studied by several researchers ([6]–[13]). In [6], the architectures of planar 3-*R*P*R* parallel mechanisms with simplified singularity loci and a procedure to determine the singularity-free workspace were proposed. This work will focus on the geometric synthesis of planar 3-*R*P*R* parallel mechanisms in order to guarantee a singularity-free workspace for a desired orientation range.

2 SINGULARITY-FREE WORKSPACE

As shown in Fig.1, a planar 3-*R*P*R* parallel mechanism with actuated prismatic joints consists of a fixed triangular base $\triangle B_1B_2B_3$ and a mobile triangular platform $\triangle P_1P_2P_3$. B_i and P_i are connected via the actuated prismatic joint of variable length $\rho_i (i = 1, 2, 3)$. Passive revolute joints are located at B_i and P_i, and the mechanism has 3 DOFs. The moving platform can translate in the xy plane and rotate with respect to an axis perpendicular to the xy plane.

Referring to Fig.1, assume, without loss of generality, that the coordinates of the attachment points of the base in the fixed frame Oxy are B_1(0,0), $B_2(t_1,0)$ and $B_3(t_2, t_3)$ and the coordinates of the attachment points of the platform in the mobile frame $O'x'y'$ are P_1'(0,0), $P_2'(t_4,0)$ and $P_3'(t_5, t_6)$. With the frames defined as shown in Fig.1, a simple singularity equation for an arbitrary

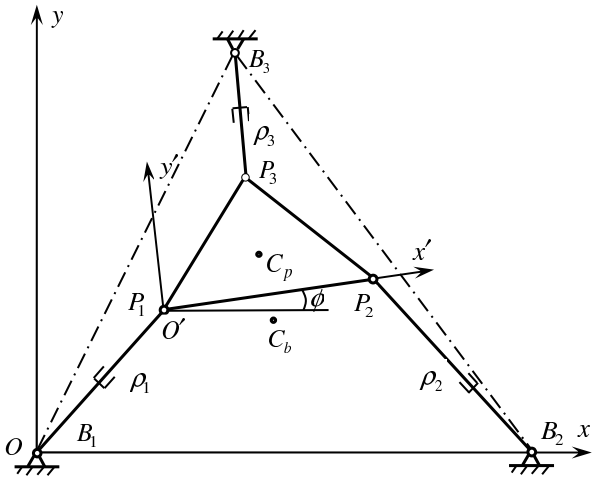

Figure 1: Planar 3-*R*P*R* parallel mechanism.

point P on the platform was derived in [6]. It takes the following form:

$$G_1x^2 + G_2y^2 + G_3xy + G_4x + G_5y + G_6 = 0, \tag{1}$$

where the coefficients $G_i(i = 1, 2, ..., 6)$ are functions of $x_p, y_p, \phi, t_1, t_2, ..., t_6$, while x_p, y_p are the coordinates of point P in the mobile frame and ϕ is the orientation angle.

In general, the singularity locus may be a hyperbola or a parabola or an ellipse [2]. Analyzing eq.(1) carefully, it can be found that when the base and the platform are similar triangles (i.e. $t_4/t_1 = t_5/t_2 = t_6/t_3 = k$, k is the size ratio between the platform and the base), $G_3 \equiv 0$ and $G_1 \equiv G_2$. In this case, the singularity locus is a circle (a special case of ellipse). This result was pointed out in [7] and can be summarized as follows: as long as the base and the platform are similar triangles, the singularity locus of any point on the platform, for a given orientation $\phi \neq i\pi(i = 0, 1)$, is a circle with centre $C(x_c, y_c)$ and radius R as follows:

$$\begin{cases} x_c = -G_4/(2G_1) = x(x_p, y_p, t_1, t_2, t_3, k, \phi), \\ y_c = -G_5/(2G_1) = y(x_p, y_p, t_1, t_2, t_3, k, \phi), \\ R = \sqrt{[G_4/(2G_1)]^2 + [G_5/(2G_1)]^2 - G_6/G_1} = R(t_1, t_2, t_3, k, \phi). \end{cases} \tag{2}$$

Eq.(2) shows that the radius of the singularity circle is independent from the position of the considered point P. When $\phi = i\pi(i = 0, 1)$, the whole plane becomes singular. This observation was used in [7] to determine the uniqueness domains of planar 3-*RPR* parallel mechanisms with similar base and platform.

Referring to [10], the workspace equations of planar 3-*RPR* parallel mechanisms can be given as

$$\begin{cases} \rho_1^2 = [x - (x_p c\phi - y_p s\phi)]^2 + [y - (x_p s\phi + y_p c\phi)]^2, \\ \rho_2^2 = [x - (x_p c\phi - y_p s\phi - t_4 c\phi + t_1)]^2 + [y - (x_p s\phi + y_p c\phi - t_4 s\phi)]^2, \\ \rho_3^2 = [x - (x_p c\phi - y_p s\phi - t_5 c\phi + t_6 s\phi + t_2)]^2 + [y - (x_p s\phi + y_p c\phi - t_5 s\phi - t_6 c\phi + t_3)]^2, \end{cases} \tag{3}$$

where $c\phi = \cos\phi, s\phi = \sin\phi$.

Actually, for a given orientation ϕ, these are three circle equations. These circles can be referred to as *workspace circles*, because they are used to determine the workspace based on the minimal and maximal values of ρ_i $(i = 1, 2, 3)$. In [6], it is verified that the three centres of the workspace circles lie exactly on the singularity circle and a procedure is proposed to determine the singularity-free workspace, as shown in Fig.2. The hatched region formed by five arcs, $M_4N_3N_3'M_5N_2M_4$, is the singularity-free workspace. The singularity-free workspace is related to the size of the inscribed circle of triangle $\triangle C_1C_2C_3$. Moreover, when the base is an equilateral triangle, this inscribed circle becomes maximal. This point can be verified as follows: for a base of unit area, the radius of the inscribed circle of triangle $\triangle C_1C_2C_3$ can be expressed as

$$r = r(t_1, t_2, k, \phi). \tag{4}$$

For a given value of k and ϕ, to obtain the maximum of r, the following conditions need to be

satisfied:

$$\begin{cases} \partial r/\partial t_1 = 0, \\ \partial r/\partial t_2 = 0, \\ \partial^2 r/\partial t_1^2 < 0, \\ \partial^2 r/\partial t_2^2 < 0. \end{cases} \tag{5}$$

For an equilateral triangle base of unit area, $t_1 = 2/\sqrt[4]{3}$, $t_2 = 1/\sqrt[4]{3}$. Substituting these values into eq.(5), it can be found that eq.(5) is satisfied.

3 ANALYSIS OF THE SINGULARITY-FREE WORKSPACE

Considering that the centroid C_p of the platform is a good representative point, this point will be taken as the considered point P in the following sections for singularity analysis. Hence, $x_p = (t_4+t_5)/3$, $y_p = t_6/3$. The area of the singularity-free workspace can be computed using the Gauss divergence theorem, provided that a description of the boundary of the workspace is available. Since the singularity-free workspace can be affected by several factors such as the orientation angle ϕ, the minimal leg length ρ_{min} as well as the shape of the base, this section analyzes the effects of these factors.

3.1 Determination of the Singularity-Free Workspace

In order to compute the area of the singularity-free workspace, the first and key step is the determination of its boundary. The boundary of the singularity-free workspace of planar 3-*RPR* parallel mechanisms can be defined with the method mentioned in [14]. Referring to Fig.2, the singularity-free workspace lies inside the singularity circle. In general, the boundary possibly consists of the arcs on six workspace circles: three circles with the minimal leg lengths $\rho_{i,min}(i = 1, 2, 3)$ and the others with the maximal leg lengths $\rho_{i,max}(i = 1, 2, 3)$. The minimal leg lengths $\rho_{i,min}$ should be

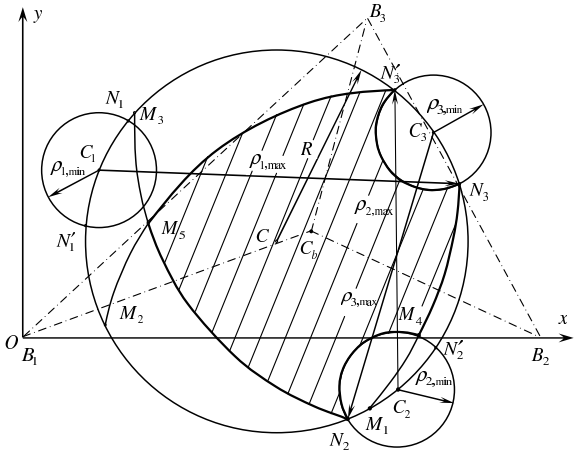

Figure 2: Singularity-free workspace.

given and the maximal leg lengths $\rho_{i,max}$ can be determined with the procedure proposed in [6]. Hence, the boundary of the singularity-free workspace can be determined as follows:

- For every workspace circle, compute the intersections with the other six circles (including the singularity circle).
- Order all of the intersections to divide the considered workspace circle into elementary arcs.
- Test each arc to see whether it lies on the boundary of the singularity-free workspace. If the considered arc lies on the boundary, the two endpoints and the middle point should satisfy the following condition:

$$\rho_{i,min} \leq d_i \leq \rho_{i,max} \qquad (i = 1, 2, 3), \tag{6}$$

  where d_i is the distance from the endpoints or the middle point of the considered arc to the centre C_i of the workspace circle.

After the boundary has been defined, the area of the singularity-free workspace can be computed using the Gauss divergence theorem [14].

3.2 Effect of the Orientation Angle

The following three cases are used for study:

Case 1: The base geometric parameters are: $t_1 = 1.8$, $t_2 = 1.2$, $t_3 = 1.11$, which form an acute triangle of unit area.

Case 2: The base geometric parameters are: $t_1 = 2/\sqrt[4]{3}$, $t_2 = 1/\sqrt[4]{3}$, $t_3 = \sqrt[4]{3}$, which form an equilateral triangle of unit area.

Case 3: The base geometric parameters are: $t_1 = 1.8$, $t_2 = 2.2$, $t_3 = 1.11$, which form an obtuse triangle of unit area.

With the algorithm proposed in Section 3.1, the area of the singularity-free workspace as a function of the orientation angle ϕ for $\rho_{min} = 0.2$ can be computed and is shown in Figs.3 and 4. Fig.3 shows that for a large range of the orientation angle, the equilateral triangle base yields the maximal singularity-free workspace. But when the orientation angle is small, Fig.4 shows that the obtuse triangle base may yield the maximal singularity-free workspace. The reason will be explained in the following subsection.

3.3 Effect of the Minimal Leg Length

If the minimal leg length ρ_{min} is constant for any orientation angle, Fig.4 shows that when the orientation angle is small, the obtuse triangle base may lead to the maximal singularity-free workspace. This is because of the effect of the minimal leg length ρ_{min}. To demonstrate this point, the area of the singularity-free workspace as a function of the minimal leg length ρ_{min} for $\phi = 45^\circ$ is computed and shown in Fig.5. This figure shows that for each case, there exists an optimal value of ρ_{min}, which leads to the maximal singularity-free workspace. When ϕ is small, the singularity circles also become small. For a constant ρ_{min}, this is equivalent to increasing the value of ρ_{min} for

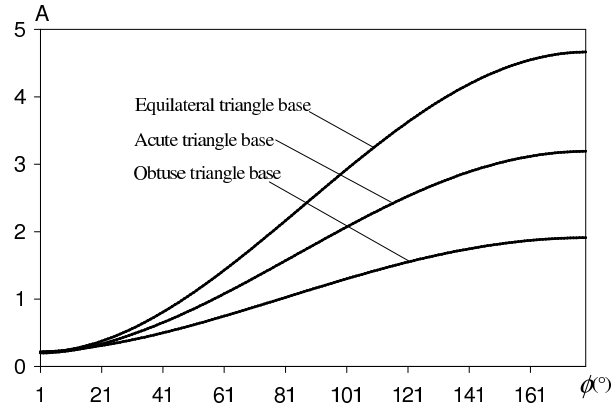

Figure 3: The area of the singularity-free workspace vs ϕ ($\rho_{min} = 0.2$).

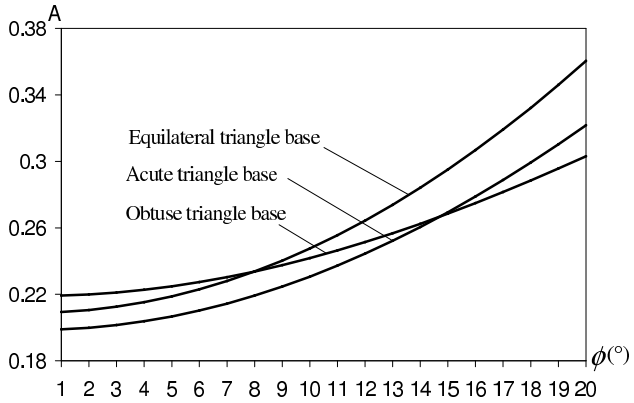

Figure 4: The area of the singularity-free workspace vs small ϕ ($\rho_{min} = 0.2$).

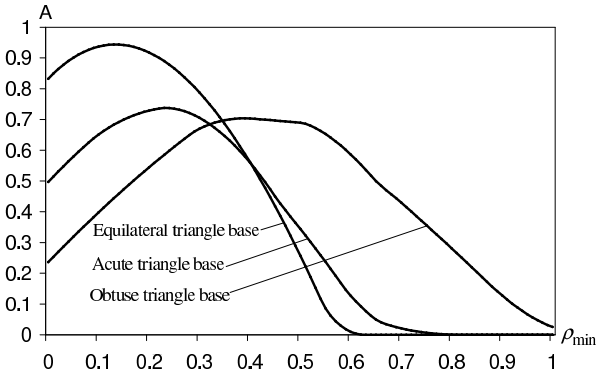

Figure 5: The area of the singularity-free workspace vs ρ_{min} ($\phi = 45°$).

unchanged singularity circles. As a result, the obtuse triangle base obtains a larger singularity-free workspace than the equilateral triangle base (see Fig.5).

To compare the singularity-free workspaces of the three cases, it should be more reasonable to

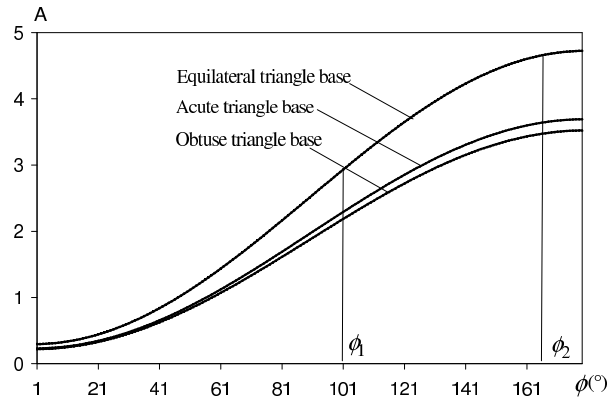

Figure 6: The area of the singularity-free workspace vs ϕ (optimal ρ_{min}).

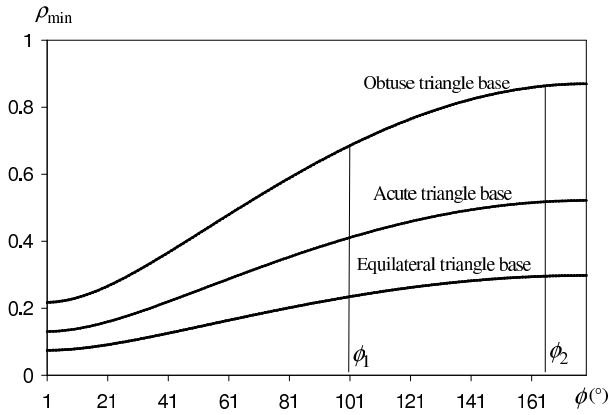

Figure 7: The optimal ρ_{min} vs ϕ.

use their respective optimal value of ρ_{min} for every ϕ. Fig.6 shows the area of the singularity-free workspace as a function of ϕ with optimal ρ_{min}. It can be seen that for any orientation angle ϕ, the equilateral triangle base always yields the maximal singularity-free workspace.

Obviously, for different orientation angles, the optimal values of ρ_{min} are different. Fig.7 shows the optimal ρ_{min} as a function of the orientation angle ϕ. It can be seen that the optimal ρ_{min} for equilateral triangle base is minimal. This is consistent with Fig.5.

3.4 Effect of the Base Shape

From the three case studies described in the previous subsections, it seems that when the base is an equilateral triangle, the planar 3-*RPR* parallel robot has the maximal singularity-free workspace. However, the following question arises: if the base assumes the shape of other acute or obtuse triangles, is this conclusion still true? In order to answer this question, consider the geometric parameter $t_1 = 2/\sqrt[4]{3}$, which is the side length of an equilateral triangle base of unit area, as a constant. Referring to Fig.1, changing t_2 leads to different base shapes. Starting from -5, with an increase of t_2, the base shape changes as follows:

obtuse triangle ($t_2 < 0$) $\rightarrow$ right triangle ($t_2 = 0$) $\rightarrow$ acute triangle ($0 < t_2 < 1/\sqrt[4]{3}$) $\rightarrow$ equilateral triangle ($t_2 = 1/\sqrt[4]{3}$) $\rightarrow$ acute triangle ($1/\sqrt[4]{3} < t_2 < 2/\sqrt[4]{3}$) $\rightarrow$ right triangle ($t_2 = 2/\sqrt[4]{3}$) $\rightarrow$ obtuse triangle ($t_2 > 2/\sqrt[4]{3}$).

The numerical results with several typical orientation angles are shown in Fig.8. This figure shows that when $t_2 = 1/\sqrt[4]{3} \approx 0.76$ (equilateral triangle base), the area of the singularity-free workspace becomes maximal. Although these results do not constitute a formal proof, they strongly support the conjecture that the equilateral triangle base provides the maximal singularity-free workspace.

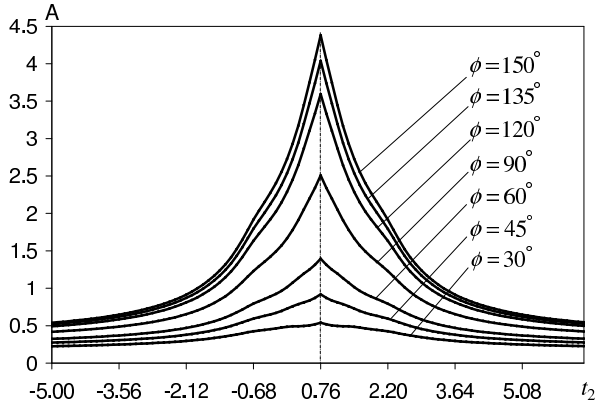

Figure 8: The area of the singularity-free workspace vs t_2.

4 GEOMETRIC SYNTHESIS

4.1 Determination of the Optimal ρ_{min} for a Prescribed Range of ϕ

In general, after a robot has been designed and manufactured, the size ratio k cannot change. But the orientation angle ϕ should cover a working range. In order to obtain the maximal singularity-free workspace, Fig.7 shows that for every value of ϕ, there exists an optimal value of the minimal leg length ρ_{min}. For a prescribed working range $\phi \in [\phi_1, \phi_2]$, it was pointed out in [6] that the radius of the singularity circle monotonically increases with ϕ. In order to avoid the singularity inside the workspace, the maximal leg lengths should be determined by ϕ_1. Fig.9 shows the construction obtained with an equilateral triangle base of unit area. The used minimal leg length is the optimal one at ϕ_1. The hatched region formed by six arcs, $N_1N_1'N_2N_2'N_3N_3'N_1$, is the singularity-free workspace at ϕ_1. However, being limited by the maximal leg length determined by ϕ_1, the singularity-free workspace at ϕ_2 is only the intercross-hatched region formed by three arcs, $M_1M_2M_3M_1$. Obviously, this workspace is much smaller than the workspace at ϕ_1. This situation shows that the optimal values of the minimal leg lengths obtained as shown in Fig.7 are not necessarily optimal for a prescribed working range of ϕ.

In order to obtain the optimal value of the minimal leg length for a prescribed working range of ϕ, six case studies are now performed. The used size ratio k is 0.6 and the prescribed working range of ϕ is $[100^\circ, 165^\circ]$, i.e., $\phi_1 = 100^\circ$ and $\phi_2 = 165^\circ$.

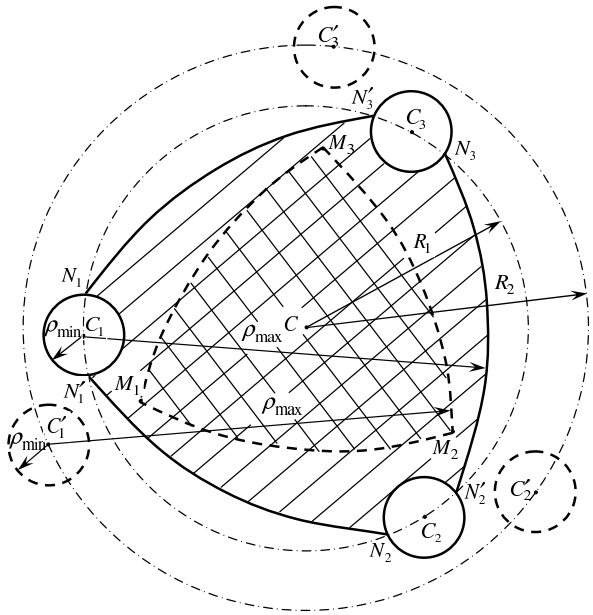

Figure 9: The singularity-free workspaces for ϕ_1 and ϕ_2 ($\phi_1 < \phi_2$).

Case 1: The minimal leg length is 0.2.
Case 2: The minimal leg length is 0.233276, which is the optimal one at ϕ_1.
Case 3: The minimal leg length is 0.295636, which is the optimal one at ϕ_2.
Case 4: The minimal leg length is determined by solving the following optimization problem:

$$\max_{\rho_{min}} A_a, \tag{7}$$

where A_a is the average area of the singularity-free workspaces over the prescribed working range of ϕ, which can be expressed as

$$A_a = \frac{1}{\phi_2 - \phi_1} \int_{\phi_1}^{\phi_2} A(\phi) d\phi. \tag{8}$$

Case 5: The minimal leg length is determined by minimizing the difference between A_1 and A_2, which are respectively the area of the singularity-free workspaces at ϕ_1 and ϕ_2, i.e.,

$$\min_{\rho_{min}} |A_1 - A_2|. \tag{9}$$

Case 6: The minimal leg length is determined by minimizing the fluctuation of the area of the singularity-free workspace, i.e.,

$$\min_{\rho_{min}} \Delta A_a, \tag{10}$$

where ΔA_a is the average difference of the area of the singularity-free workspaces with respect to A_a, given as

$$\Delta A_a = \frac{1}{n} \sum_{i=1}^{n} |A_i - A_a|, \tag{11}$$

Table 1: Numerical results of the case studies.

$Case$	ρ_{min}	ρ_{max}	A_1	A_2	$\lvert A_1 - A_2 \rvert$	A_a	ΔA_a
1	0.2	1.995261	2.887449	1.523389	1.364060	2.088205	0.368054
2	0.233276	2.009044	2.894137	1.589744	1.304393	2.146203	0.354989
3	0.295636	2.033677	2.871123	1.711608	1.159515	2.234786	0.314177
4	**0.412168**	**2.075469**	**2.709505**	**1.927286**	**0.782219**	**2.308779**	**0.207856**
5	**0.647965**	**2.142531**	**1.957423**	**1.957423**	**0**	**2.012230**	**0.024850**
6	0.656267	2.144448	1.921667	1.947769	0.026102	1.992113	0.024325

where A_i is the area of the singularity-free workspace at ϕ_i.

If the convergence precision is set to 10^{-6}, n in eq.(11) will be greater than 400. The numerical results are shown as Fig.10 and listed in Table 1. The results show that for cases 1–3, the differences between A_1 and A_2 as well as the values of ΔA_a are quite large. For case 4, the difference between A_1 and A_2 as well as the value of ΔA_a decrease much, and A_a reaches the maximum. Hence, if the objective of the designers is to obtain the maximal singularity-free workspace over a prescribed range of ϕ, case 4 is the optimal solution.

For case 5, $A_1 = A_2$ and ΔA_a is only 0.024850, which is quite small. For case 6, the value of ΔA_a reaches the minimum, 0.024325. Fig.10 shows that the graphs corresponding to cases 5 and 6 are very close. However, the graph corresponding to case 5 is always above that corresponding to case 6. Hence, the value of the A_a in case 5 is larger than that in case 6, while the value of the ΔA_a in case 5 is very close to that in case 6. Especially, the difference between A_1 and A_2 in case 5 is 0. Hence, if the objective of the designers is to obtain a singularity-free workspace of almost the same size at every orientation angle in the prescribed range, case 5 is the optimal solution.

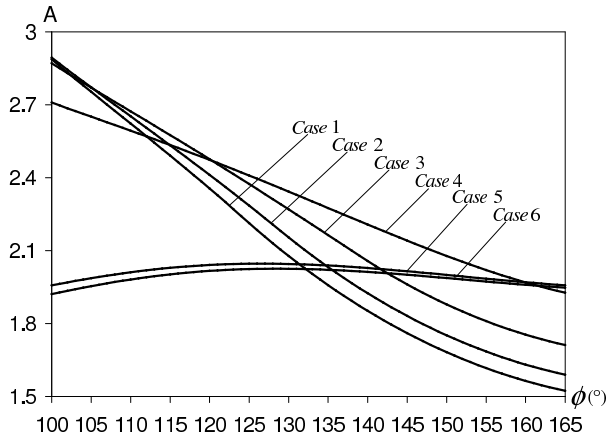

Figure 10: The area of the singularity-free workspace vs ϕ (with different ρ_{min}).

4.2 Synthesis Procedure

In order to guarantee a singularity-free workspace for a desired orientation range, the procedure of the geometric synthesis of planar 3-*RPR* parallel mechanisms can be generalized as follows:

- Select a proper size ratio k between the platform and the base.
- According to the desired function, determine a range of the orientation angle: $[\phi_1, \phi_2]$. Note that $\phi = i\pi (i = 0, 1)$ should not be included in the prescribed range since these values correspond to singular orientations.
- Use eq.(7) or (9) (depending on which design objective is pursued) to compute the optimal minimal leg length. When the minimal leg length is available, the maximal leg length at ϕ_1 can be determined using the approach mentioned in Section 3.1. To avoid singularity inside the workspace, this determined maximal leg length is also used as the maximal leg length for the whole prescribed range of ϕ.
- Choose a proper leg length range within the computed maximal leg length range for each leg and complete the geometric design. Take case 4 as an example, the computed maximal leg length range is [0.412168, 2.075469]. A proper leg length range can be taken as [1, 1.5], which will guarantee a singularity-free workspace for the desired orientation range $[100^\circ, 165^\circ]$.

5 CONCLUSIONS

This work focuses on the geometric synthesis of planar 3-*RPR* parallel mechanisms in order to guarantee a singularity-free workspace for a desired orientation range. The effects of the orientation angle, the minimal leg length as well as the base shape on the singularity-free workspace are analyzed using the Gauss divergence theorem. The results show that for every orientation angle, there exists an optimal minimal leg length which leads to the maximal singularity-free workspace. If the optimal minimal leg lengths are used, the equilateral triangle base yields the maximal singularity-free workspace for any orientation angle. However, for a prescribed working range of the orientation angle, the optimal minimal leg length may be different from the individual optimal minimal leg lengths. Based on the optimal minimal leg length determined for a prescribed working range of the orientation angle, a geometric synthesis procedure is proposed in order to guarantee a singularity-free workspace. Although the proposed synthesis procedure is based on an equilateral triangle base, it can also be applied to the geometric synthesis of planar 3-*RPR* parallel robots with general similar base and platform.

Acknowledgements The authors would like to acknowledge the financial support of the Natural Sciences and Engineering Research Council of Canada (NSERC) as well as the Canada Research Chair (CRC) Program.

REFERENCES

[1] Gosselin, C., and Angeles, J., 1990, "Singularity Analysis Of Closed-Loop Kinematic Chains". IEEE Transactions on Robotics and Automation **6**(3), pp.281–290.

[2] Sefrioui, J., and Gosselin, C., 1995, "On The Quadratic Nature of The Singularity Curves of Planar Three-Degree-of-Freedom Parallel Manipulators", Mechanism and Machine Theory, **30**(4), pp.533–551.

[3] Collins, C.L. and McCarthy, J.M., 1998, "The Quartic Singularity Surfaces of Planar Platforms in The Clifford Algebra of The Projective Plane", Mechanism and Machine Theory, **33** (7), pp.931–944.

[4] Mayer St-Onge, B. and Gosselin, C., 2000, "Singularity Analysis and Representation of The General Gough-Stewart Platform", International Journal of Robotics Research, **19**(3), pp.271–288.

[5] Jiang, Q., and Gosselin, C., 2008, "Singularity Equations of Gough-Stewart Platforms Using a Minimal Set of Geometric Parameters", ASME Journal of Mechanical Design, 130(11), 112303.

[6] Jiang, Q., and Gosselin, C., 2008, "Geometric Optimization of Planar 3-RPR Parallel Mechanisms", Transactions of the Canadian Society for Mechanical Engineering, 31(4), pp.457-468.

[7] Kong, X, and Gosselin, C., 2000, "Determination of The Uniqueness Domains of 3-*RPR* Planar Parallel Manipulators With Similar Platforms", Proceedings of ASME 2000 Design Engineering Technical Conferences and Computers and Information in Engineering Conference, Baltimore, Maryland, Sept.10-13.

[8] Gosselin, C., and Angeles, J., 1988, "The Optimum Kinematic Design of A Planar Three-Degree-of-Freedom Parallel Manipulator", Journal of Mechanisms, Transmissions, and Automation in Design, **110**, pp.35–41.

[9] Liu, X.J., Wang, J., and Gao, F., 1996, "Performance of The Workspace for Planar 3-DOF Parallel Manipulators". Robotica, **18**, pp.563–568.

[10] Gosselin, C., and Jean, M., 1996, "Determination of The Workspace of Planar Parallel Manipulators With Joint Limits", Robotics and Autonomous Systems, **17**, pp.129–138.

[11] Merlet, J.P., 1996, "Direct Kinematics of Planar Parallel Manipulators", Proceedings of the IEEE International Conference on Robotics and Automation, April 22-28, pp.3744–3749.

[12] Gallant, M., and Boudreau, R., 2002, "The Synthesis of Planar Parallel Manipulators With Prismatic Joints for An Optimal, Singularity-Free Workspace", Journal of Robotics Systems, **19**(1), pp.13–24.

[13] Arsenault, M., and Boudreau, R., 2006, "Synthesis of Planar Parallel Mechanisms While Considering Workspace, Dexterity, Stiffness and Singularity Avoidance", ASME Journal of Mechanical Design, **128**(1), pp.69–78.

[14] Gosselin, C., and Guillot, M., 1991, "The Synthesis of Manipulators With Prescribed Workspace", ASME Journal of Mechanical Design, **113**, pp.451–455.